FIML for Channel flow (Spalart-Allmaras turbulence model)

Vishal Srivastava

Field inversion and Machine Learning framework has been used here to augment Spalart-Allmaras model to obtain correct profiles for Channel flow. Different augmentation strategies have been proposed along with a few results. Let us first summarize the development of the Spalart-Allmaras (SA) model.

The SA model has been calibrated using the results from fully developed mixing layers, far wake, and zero pressure gradient (ZPG) boundary layer (B/L) at $Re = 10^4$. The development goes as follows:

- Take a Spalart-Allmaras working variable, $\widetilde{\nu}$, and consider it to be the same as eddy viscosity (ν_t) for the time being. The need for this term will be addressed in a bit. Similarly, define a variable, $\widetilde{\Omega}$, and consider it to be equal to the vorticity magnitude (Ω) for now.
- The source term for turbulence production is modeled as the product of eddy viscosity ($\widetilde{\nu}$) and the vorticity magnitude ($\widetilde{\Omega}$) scaled by an appropriate coefficient (c_{b1}). Thus, mathematically,
$$\mathcal{P} = c_{b1}\widetilde{\nu}\widetilde{\Omega}$$
- It is assumed that the eddy viscosity (ν_t) diffuses and is cross-produced/dissipated based on a traditional conservative diffusion term, $\dfrac{1}{\sigma}\nabla\cdot((\nu+\widetilde{\nu})\nabla\widetilde{\nu})$, and a non-conservative diffusion term, $\dfrac{c_{b2}}{\sigma}(\nabla\widetilde{\nu})^2$. A basic mathematical analysis using the transport equation
$$\frac{D\widetilde{\nu}}{Dt} = \mathcal{D}, \qquad \text{where} \quad \mathcal{D} = \frac{1}{\sigma}\nabla\cdot((\nu+\widetilde{\nu})\nabla\widetilde{\nu}) + \frac{c_{b2}}{\sigma}(\nabla\widetilde{\nu})^2$$
quickly shows that the integral of quantity $\widetilde{\nu}^{1+c_{b2}}$ over a large enough flow domain must remain conserved under the assumption that $\widetilde{\nu}^{1+c_{b2}}\nabla\widetilde{\nu}$ has a finite support (which, roughly, is always the case). There is a fair bit of analysis on the constraints on c_{b2} and $\dfrac{1+c_{b2}}{\sigma}$ which is being skipped for now.
- Using just these terms, possible coefficient values for c_{b1}, c_{b2} and σ are obtained by calibrating these against the free shear flow results from the fully developed mixing layer and far wake.
- Now, we move on to the next part of the model. Firstly, let us assume that the log layer is uncompromisable for high Reynolds numbers. In this case, using dimensional analysis one has the destruction term as $-c_{w1}\dfrac{\widetilde{\nu}^2}{d^2}$, where, to ensure log law, $c_{w1} = \dfrac{c_{b1}}{\kappa^2} + \dfrac{1+c_{b2}}{\sigma}$.
- This dissipation term is overly so in the outer layer resulting in an underestimation of the friction coefficient for the ZPG B/L case. A correction function f_w is thus multiplied to the dissipation term such that it equals unity in the log layer. The definition of log layer has been set to $r = \dfrac{\widetilde{\nu}}{\widetilde{\Omega}\kappa^2 d^2} = 1$ based on which the function f_w is defined as follows.
$$f_w = g\left(\frac{1+c_{w3}^6}{g^6+c_{w3}^6}\right)^{1/6}, \qquad \text{where} \quad g = r + c_{w2}(r^6 - r)$$
Two possible log layer preserving model augmentations in this step are mentioned as follows and have been named c_{w2}-augmentation and f_w-augmentation
$$c_{w2}\text{-augmentation:} \qquad c_{w2}^{\text{aug}} = \beta_1^{\text{FIML}}\left(r, \frac{\widetilde{\nu}\widetilde{\Omega}}{\tau_w^{\text{SA}}}\right)c_{w2}$$
This comes in directly from the observation that the coefficient c_{w2} was calibrated based on the ZPG B/L case at $Re = 10^4$ and might be different for different flows and so, will be the first preference for augmentation to correct wall shear stress values. Here, τ_w^{SA} is the wall shear stress evaluated based on the solutions from the baseline SA model.
$$f_w\text{-augmentation:} \qquad f_w^{\text{aug}} = \beta_2^{\text{FIML}}\left(r, \frac{\widetilde{\nu}\widetilde{\Omega}}{\tau_w^{\text{SA}}}\right)(f_w - 1) + 1$$

This augmentation strategy sits a level above the previous one and can be used to correct the functional form of f_w if needed. It is a rather simple and consistent solution as when $\beta = 1$, f_w remains unperturbed and in the log layer, where $f_w = 1$, the new value, $f_w^{\text{aug}} = 1$.

- Finally, focusing on the near wall behaviour, a transformation is applied to $\widetilde{\nu}$ such that it is $\kappa y u_\tau$ (same as the linear relation for the log layer) until the log layer and ν_t outside the inner layer. A similar transformation is needed between $\widetilde{\Omega}$ and Ω to ensure the constant shear in and below the log layer. The following transformations have been defined for this purpose.

$$\nu_t = \widetilde{\nu} f_{v1}, \qquad f_{v1} = \frac{\chi^3}{\chi^3 + c_{v1}^3}, \qquad \chi = \frac{\widetilde{\nu}}{\nu}$$

$$\widetilde{\Omega} = \Omega + \frac{\widetilde{\nu}}{\kappa^2 d^2} f_{v2}, \qquad f_{v2} = 1 - \frac{\chi}{1 + \chi f_{v1}}$$

Here again, we get a chance to augment the model without meddling with any existing calibrations or the log layer. The following augmentation seems to work very well in correcting the buffer layer as shown in the results from channel flow configurations later in the document.

$$\chi^{\text{aug}} = \beta_3^{\text{FIML}} \left(\frac{\nu}{\nu_t + \nu} \right) \chi$$

The following types of augmentation have been attempted:

1. $c_{w2}^{\text{aug}} = \beta \left(r, \quad \dfrac{\widetilde{\nu}\widetilde{\Omega}}{\tau_w^{\text{SA}}} \right) c_{w2}$

2. $f_w^{\text{aug}} = \beta \left(r, \quad \dfrac{\widetilde{\nu}\widetilde{\Omega}}{\tau_w^{\text{SA}}} \right) f_w$

3. $f_{v1}^{\text{aug}} = \beta \left(\dfrac{\nu}{\nu_t + \nu} \right) f_{v1}$

4. $\mathcal{P}^{\text{aug}} = \beta \left(\dfrac{\kappa^2 d^2}{\nu} \dfrac{\partial u}{\partial y}, \quad \dfrac{\kappa^3 d^3}{\nu} \dfrac{\partial^2 u}{\partial y^2}, \quad \dfrac{\widetilde{\nu}\widetilde{\Omega}}{\tau_w^{\text{SA}}} \right) \mathcal{P} \qquad$ where $\mathcal{P} = $ Production

The results for the 1st and 2nd kind of augmentation are similar in this particular case.

Results

FIML-Classic augmentation of the 3rd kind

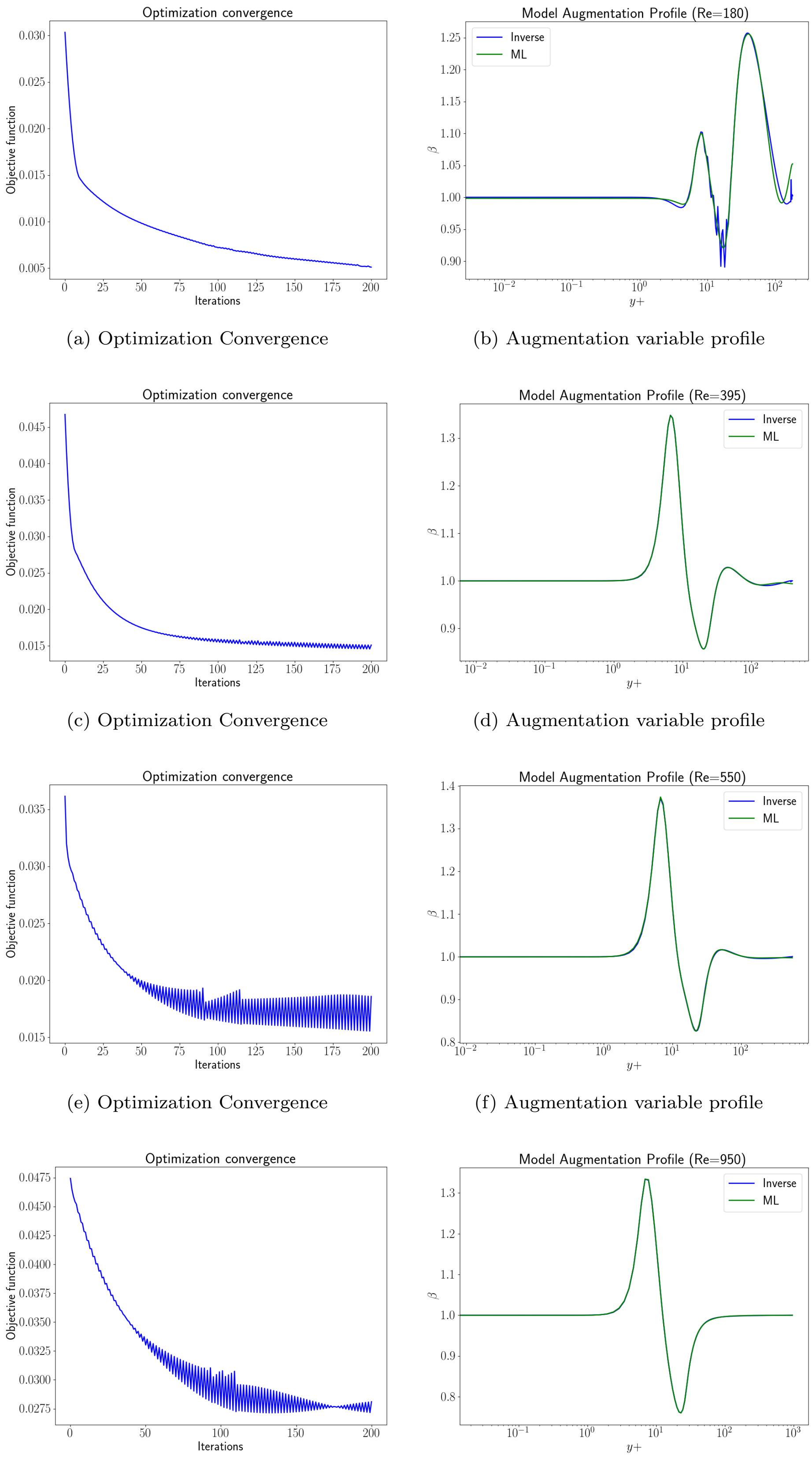

(a) Optimization Convergence

(b) Augmentation variable profile

(c) Optimization Convergence

(d) Augmentation variable profile

(e) Optimization Convergence

(f) Augmentation variable profile

(g) Optimization Convergence

(h) Augmentation variable profile

Figure 1: Convergence and beta plots

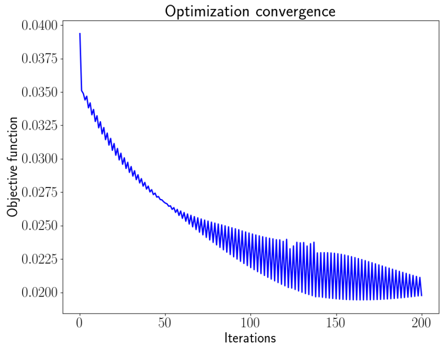

(a) Optimization Convergence

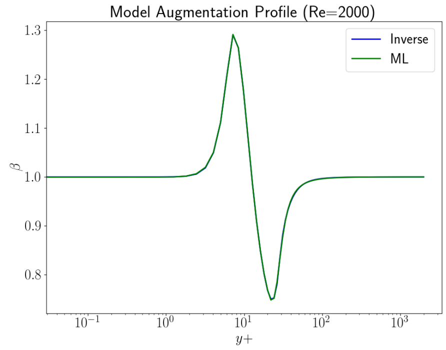

(b) Augmentation variable profile

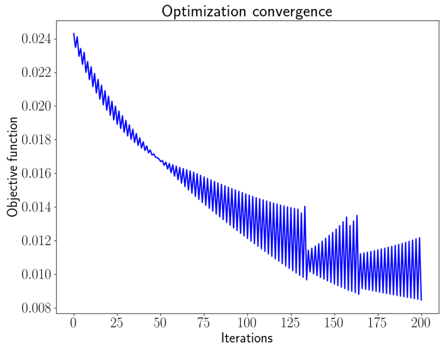

(c) Optimization Convergence

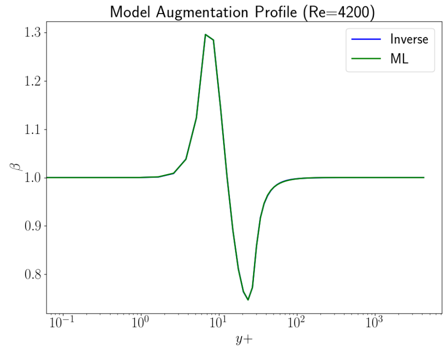

(d) Augmentation variable profile

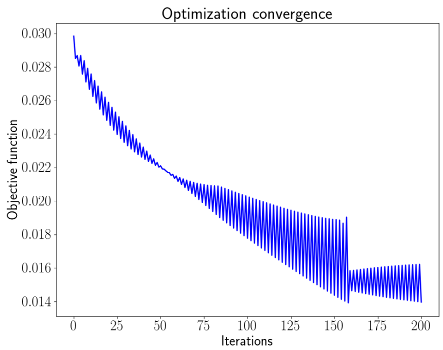

(e) Optimization Convergence

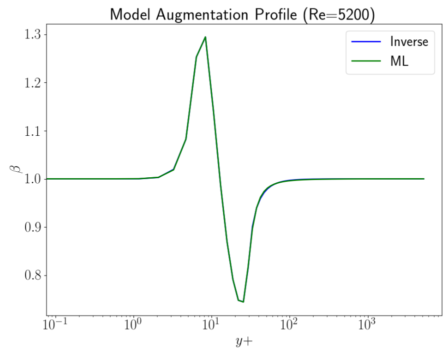

(f) Augmentation variable profile

Figure 2: Convergence and beta plots

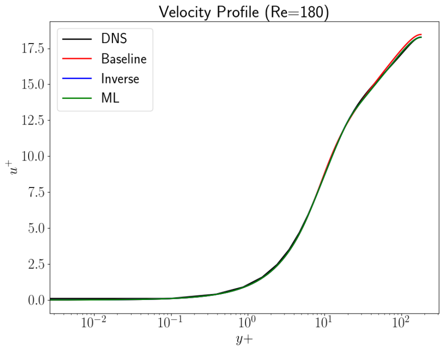

(a) Velocity profile

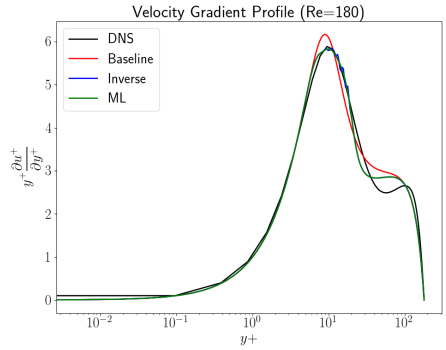

(b) Velocity Gradient profile

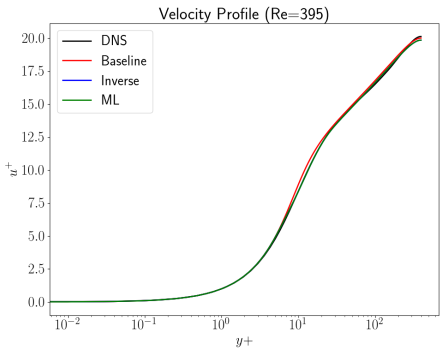

(c) Velocity profile

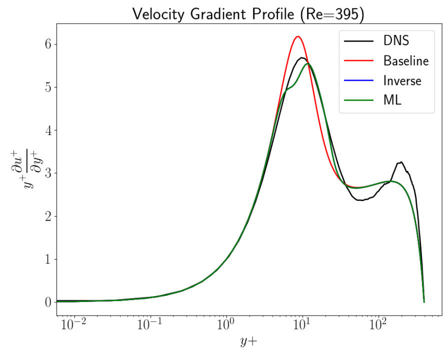

(d) Velocity Gradient profile

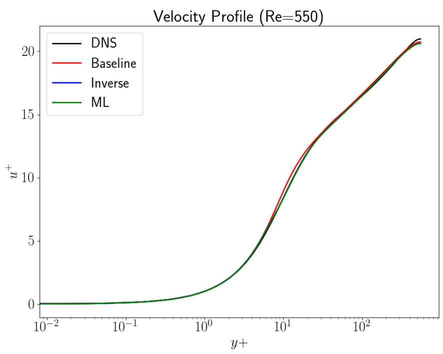

(e) Velocity profile

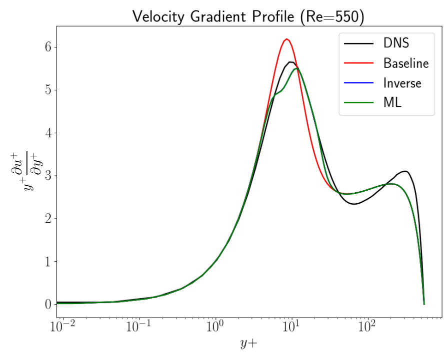

(f) Velocity Gradient profile

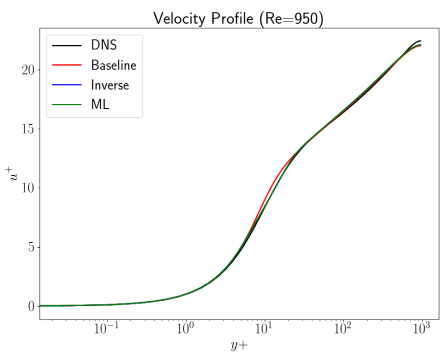

(g) Velocity profile

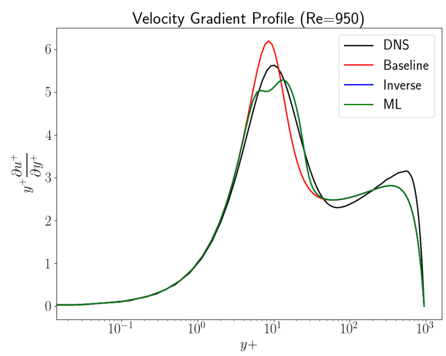

(h) Velocity Gradient profile

Figure 3: Velocity and Velocity Gradient Profiles

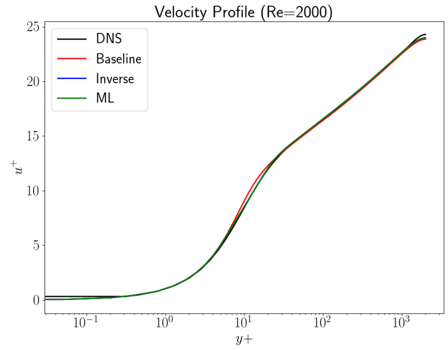

(a) Velocity profile

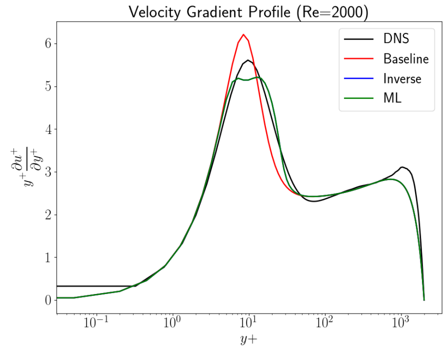

(b) Velocity Gradient profile

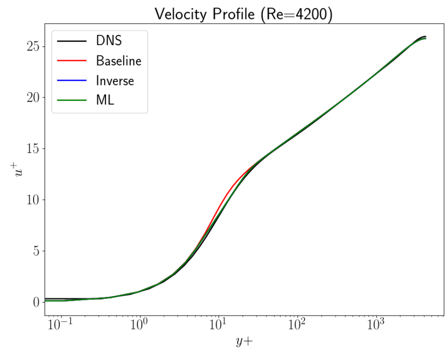

(c) Velocity profile

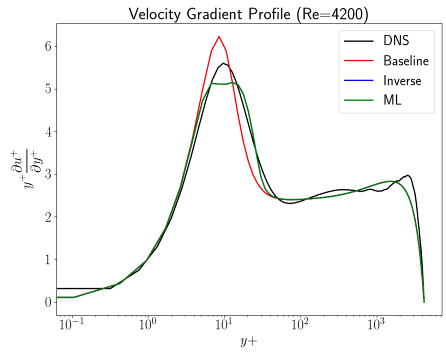

(d) Velocity Gradient profile

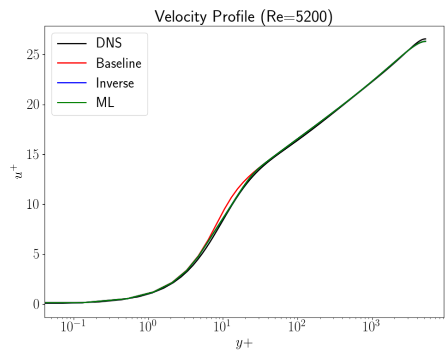

(e) Velocity profile

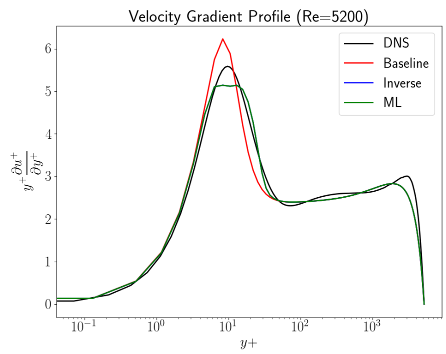

(f) Velocity Gradient profile

Figure 4: Velocity and Velocity Gradient Profiles

Note here that the beta profiles are almost identical in the y^+ (wall) coordinates, which means that the correction is nearly constant across Reynolds numbers.

FIML-Classic augmentation of the 1st kind

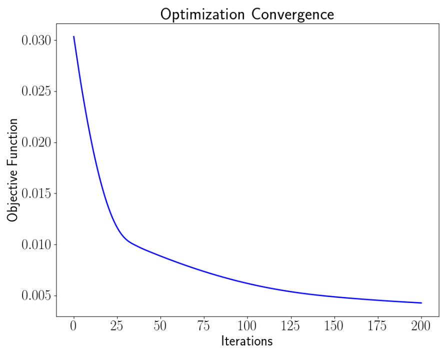

(a) Optimization Convergence

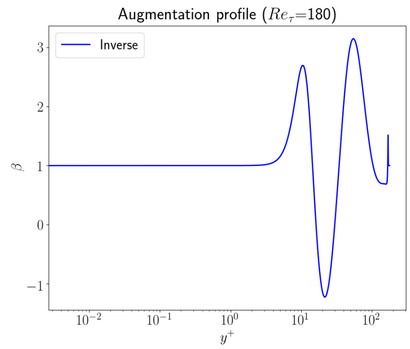

(b) Augmentation variable profile

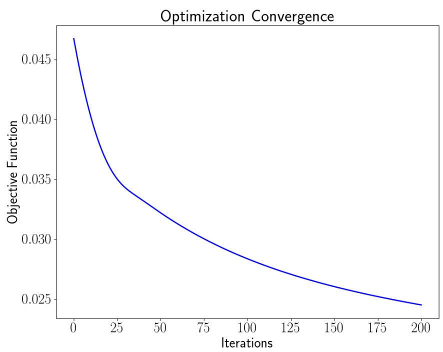

(c) Optimization Convergence

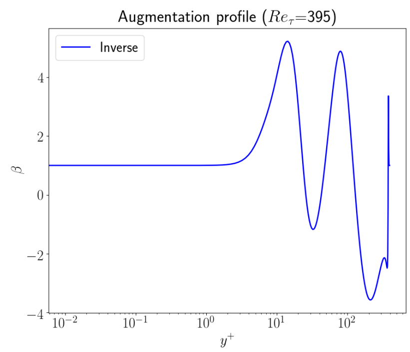

(d) Augmentation variable profile

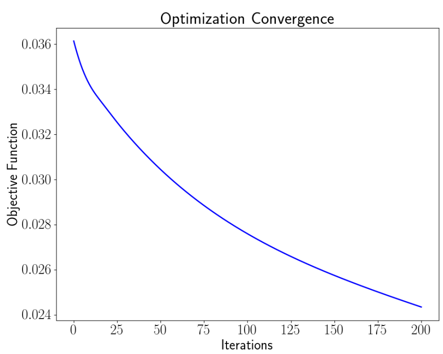

(e) Optimization Convergence

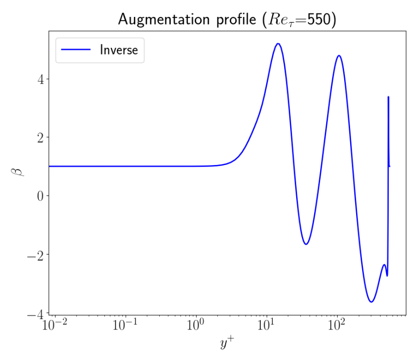

(f) Augmentation variable profile

Figure 5: Convergence and beta plots

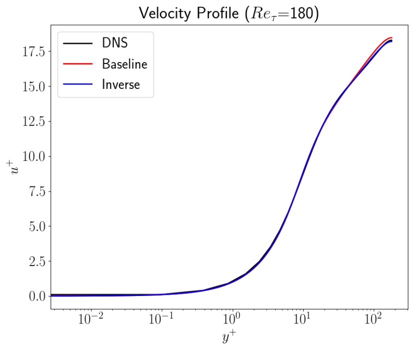

(a) Velocity profile

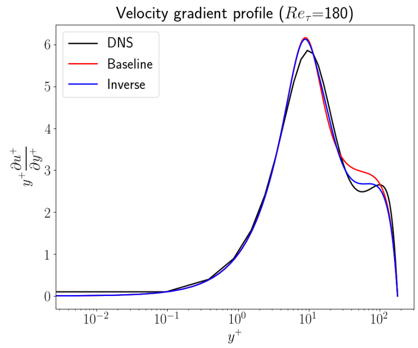

(b) Velocity Gradient profile

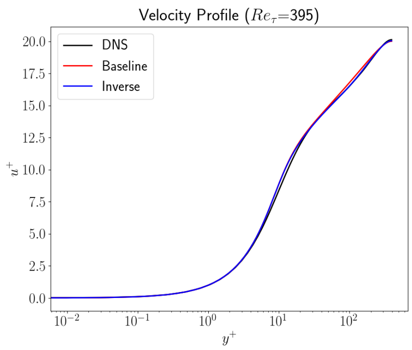

(c) Velocity profile

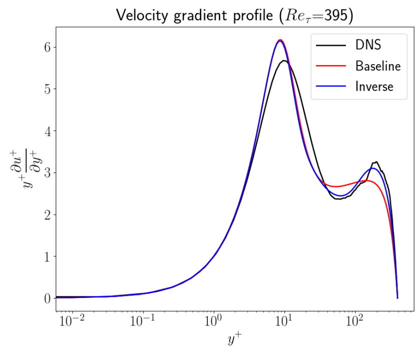

(d) Velocity Gradient profile

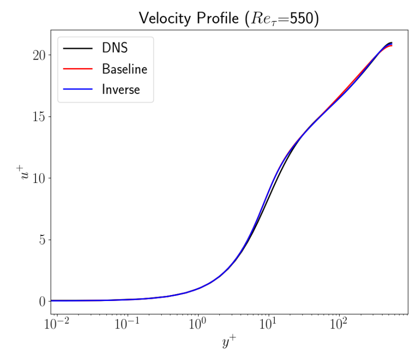

(e) Velocity profile

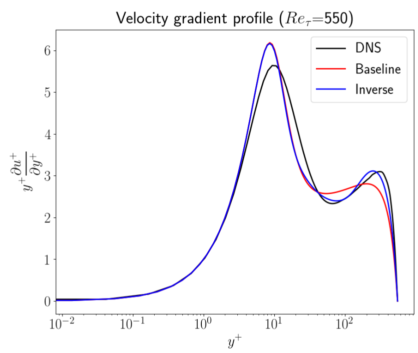

(f) Velocity Gradient profile

Figure 6: Velocity and Velocity Gradient Profiles

As can be seen in the above plots, since the major discrepancy here is in the buffer layer, this augmentation struggles to correct the profile as well as the previous one and shows large and even negative values for the augmentation factor. Hence, it will be much efficient to correct the terms individually for the zones that need to be corrected.

FIML-Classic augmentation of the 4th kind

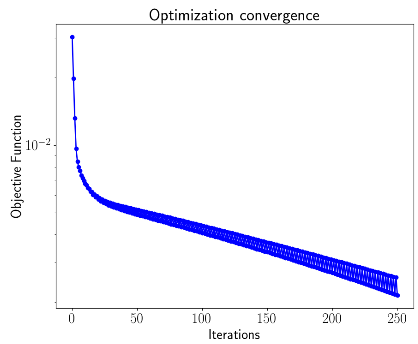

(a) Optimization Convergence

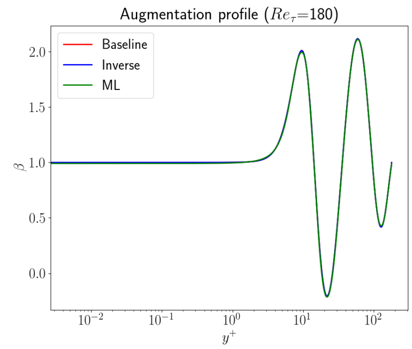

(b) Augmentation variable profile

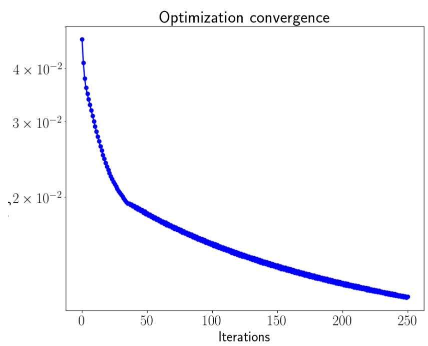

(c) Optimization Convergence

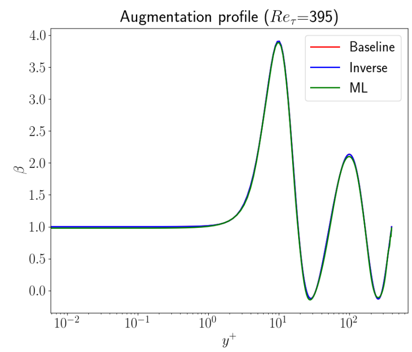

(d) Augmentation variable profile

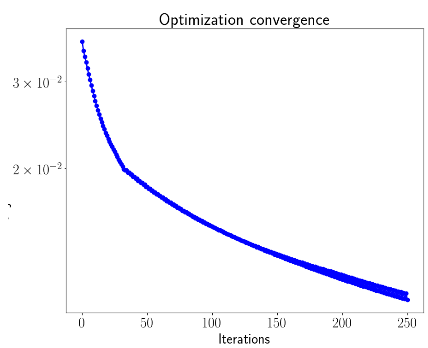

(e) Optimization Convergence

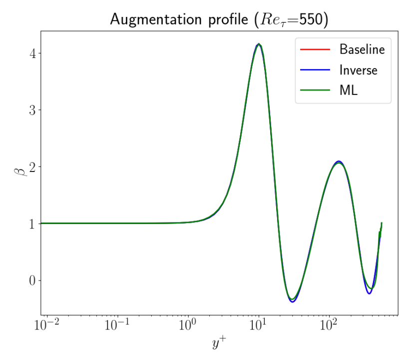

(f) Augmentation variable profile

Figure 7: Convergence and beta plots

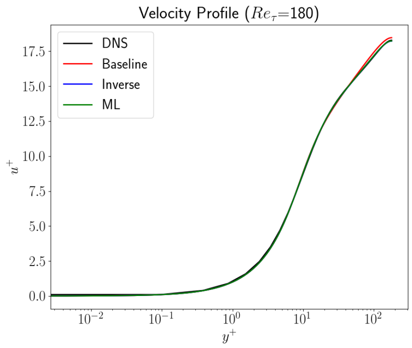

(a) Velocity profile

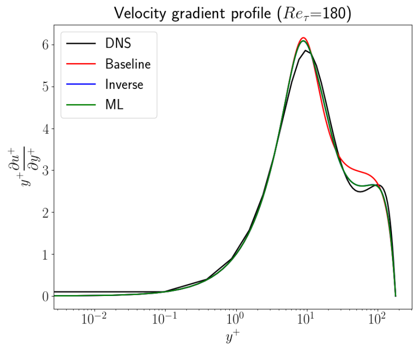

(b) Velocity Gradient profile

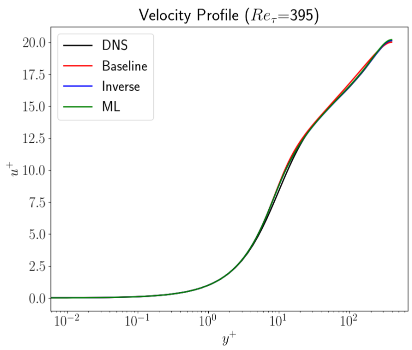

(c) Velocity profile

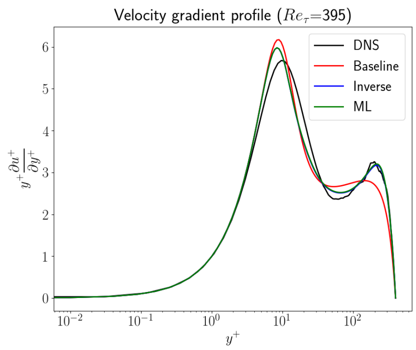

(d) Velocity Gradient profile

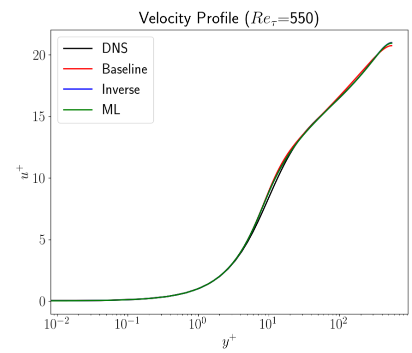

(e) Velocity profile

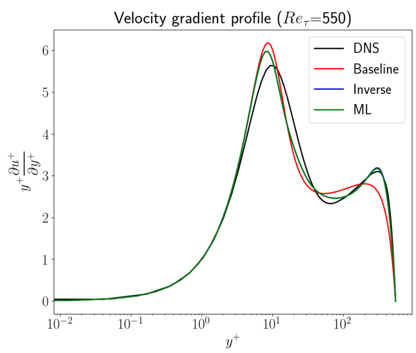

(f) Velocity Gradient profile

Figure 8: Velocity and Velocity Gradient Profiles

Here too, the optimization tries to correct the buffer layer but isn't successful and leads to β values of a large magnitude than expected. Also, this augmentation neither respects the original calibration nor the law of the wall.